Analysis of the hygroscopic and hygroelastic behaviours of water aged flax-epoxy composite

Belahcen Djellouli, Wajdi Zouari, Mustapha Assarar, Rezak Ayad

Version of Record: https://www.sciencedirect.com/science/article/pii/S0263822321001537
Manuscript_1e2e1d497cde99325811a59b676ce9c2

Analysis of the hygroscopic and hygroelastic behaviours of water aged flax-epoxy composite

Belahcen Djellouli *, Wajdi Zouari, Mustapha Assarar, Rezak Ayad

University of Reims Champagne Ardenne, ITheMM EA 7548, 51097 Reims, France

Abstract

In this paper, an analysis of the hygroscopic and hygroelastic behaviours of unidirectional flax fibre-reinforced epoxy composite is presented. Samples of this composite material were elaborated by the vacuum infusion process, then cut and prepared to be aged in tap water until saturation. To describe their hygroscopic behaviour, Fick's model is considered and an optimisation procedure is developed to identify their macroscopic water diffusion parameters. After that, a plane finite element modelling of the hygroscopic behaviour of the aged flax-epoxy samples is conducted to identify the flax fibre radial and longitudinal water diffusion parameters using an inverse approach. Finally, a plane finite element analysis of their hygroelastic behaviour is proposed allowing the estimation of the hygroscopic internal stress in flax fibres and epoxy matrix. In particular, the hygroscopic analysis reveals that water diffusion is more pronounced in the direction of flax fibres compared to the transverse and thickness directions. In addition, the hygroelastic finite element modelling highlights the high compressive and tensile stress subjected to flax fibres and epoxy matrix, respectively, due to water absorption.

Keywords: Flax-epoxy composite; water ageing; Fick's model; hygroscopic and hygroelastic finite element analysis; internal stress.

1. Introduction

Natural fibre reinforced polymer composites gain ground in several sectors such as automotive and construction. This increased use of these materials is motivated by the interesting specific mechanical properties of natural fibres as well as their several advantages related particularly to the environmental impacts [1–7]. Indeed, natural fibres are renewable resources, biodegradable, neutral in terms of CO_2 emissions and require relatively low energy to be produced [2]. However, the anisotropic nature of natural fibres and their high sensitivity to the surrounding environment conditions, especially humidity (a natural fibre swells and shrinks in presence of moisture) and temperature, constitute a major barrier to their wide development. Accordingly, many works have investigated the effect of humidity on the

* Corresponding author. Tel.: +33 325427152; fax: +33325427098
E-mail address: belahcen.djellouli@etudiant.univ-reims.fr

mechanical and dynamic characteristics of natural fibre-reinforced polymer composites [8–19]. They have principally shown that the elastic and failure properties of these materials significantly vary with the surrounding environment, which consequently reduces their durability.

In order to promote the use of natural fibre-reinforced polymer materials in environmental conditions, it is essential to understand their moisture diffusion kinetics. Some physical models that can describe this phenomenon, particularly Fick's and Langmuir's models [20,21], have been considered in the literature. For natural fibre-reinforced composites, the one-dimensional (1D) Fick's model has been mainly used to identify their moisture diffusion parameters [6,11,14,18,22–26]. For example, in the work by Christian and Billington [22], the approximation of Shen and Springer has been considered to calculate the 1D diffusion parameters of hemp/cellulose acetate (hemp-cellulose) and hemp/poly (β-hydroxybutyrate) composites (hemp-PHB) under various moisture and temperature conditions. In particular, these authors have found that the moisture diffusion parameters of hemp-cellulose and hemp-PHB composites, hygrothermal aged at 30°C and 100% relative humidity (RH), are respectively 20 and 10 times that of glass-polyester composite. Recently, Cheour et al. [26] have analysed the impact of water ageing on the free vibration behaviour of flax-glass hybrid composites. The authors have supposed that water diffusion is carried out exclusively along the thickness direction of the composite samples and used Fick's 1D model to identify their diffusion parameters. They have found that the position of the flax layers in the hybrid laminates directly affects the values of the flexural modulus, the loss factor and the mass gain at saturation. In addition, the flexural modulus of the aged flax-glass hybrid composite is found 4.5 times higher than that of the aged flax composite.

Moisture diffusion in natural fibre-reinforced composite materials depends on various parameters among others the temperature [22,27,28], the type of natural fibres and their morphology [29,30] . These parameters indicate that moisture diffusion is a rather complex phenomenon which could not be only described by 1D Fick's model. For this purpose, it is necessary to consider a three-dimensional (3D) analysis that allows describing moisture diffusion in the three directions. 3D moisture diffusion analyses have been mainly considered in synthetic fibre-reinforced polymer composites [31–37]. However, only a few works have studied moisture diffusion in natural fibre-reinforced composites by considering 3D diffusion models. For example, Saidane et al. [8] have shown that 3D Fick's model accurately describes water diffusion kinetics in flax-epoxy composite. Their results have also shown that water

diffusion mainly occurs in the direction of the flax fibres and their morphology has an impact on the composite behaviour. Recently, Chilali et al. [30] have assessed the main 3D water diffusion parameters of twill flax fabric-reinforced thermoplastic and thermoset composites, aged in tap water until saturation, by considering Fick's and Langmuir's 3D models. In particular, they have found that the mass at saturation of the aged composite specimens increases linearly with fibre orientation and decreases with thickness.

Usually, the analytical models can only describe moisture diffusion in composite materials at the macroscopic scale. In addition, these analytical models can't predict the diffusion behaviour of composite constituents such as the moisture diffusion properties of natural fibres, which are relatively difficult to measure experimentally. The use of a numerical finite element model can be considered as an alternative to overcome the experimental difficulties, but the literature reveals a limited number of contributions dealing with the numerical modelling of moisture diffusion in natural fibre-reinforced composites. Among these contributions, Regazzi et al. [28] have modelled water diffusion in Polylactic acid (PLA) composite specimens reinforced with dog bone-shaped short flax fibres. The numerical model has considered the PLA-flax composite samples as homogeneous materials. Homogeneous numerical modelling has also been considered by Péron et al. [38] to describe moisture diffusion and hygroscopic swelling in flax-polypropylene composite. Contrary to these homogeneous finite element models, Chilali et al. [39] have considered the heterogeneity of twill flax fabric-reinforced epoxy composites by using two geometric [0/90] and elliptical models to describe the waviness of the flax fabrics. The authors have estimated the radial water diffusion coefficient of the flax fibre by modelling the hygroscopic behaviour of the aged flax-epoxy samples. In another study, Zouari et al. [40] have developed a three-node triangular plane finite element to analyse the hygroscopic behaviour of 2/2 twill flax fabric-reinforced epoxy composite aged in tap water at room temperature. To take account of the heterogeneity of the flax-epoxy composite in the finite element model, they have considered a sinusoidal description of the flax fabric undulation. They have shown that water diffusion coefficients of the epoxy matrix and the flax fibre follow an exponential evolution as a function of the composite thickness.

In addition to the hygroscopic behaviour, the finite element analysis has been also considered to estimate the internal stress induced by moisture absorption especially in synthetic fibre-reinforced composites [41–47]. The number of contributions dealing with the estimation of internal hygroscopic stress in natural fibre-reinforced composite remains limited in the

literature [38,39]. Péron et al. [38] have developed a hydromechanical model based on the finite difference method, where the diffusion problem is first solved, which allows determining the distribution of water content in unidirectional flax-polypropylene laminate samples. Then, the mechanical problem is solved by taking into account the hygroscopic swelling due to the previously calculated water content. They have found that most of the plies (about 75% of the entire laminate) are subjected to compressive stress across the transverse direction of the flax fibres. Chilali et al. [39] have considered the temperature-displacement analogy in their finite element model to estimate the internal stress induced by hygroscopic swelling in flax-epoxy samples. In particular, they have shown the high stress concentration at the fibre/matrix interface induced by the dissimilar swelling between the flax fibres and the epoxy matrix. Stress concentration peaks reaching 300 MPa have been estimated which greatly exceed the ultimate tensile strength of the flax-epoxy specimens.

Most of the above-cited works have been interested only in the estimation of the flax fibre radial moisture diffusion coefficient. Moreover, some of these studies have considered the temperature-displacement analogy to estimate the hygroscopic internal stress. In the continuation of these works, an estimation of the flax fibre radial and longitudinal moisture diffusion coefficients is given in this contribution by combining numerical and experimental results of water aged flax-epoxy specimens. In addition to that, a three-node triangular hygroelastic membrane finite element is proposed to analyse the hygroelastic behaviour of the studied materials. This finite element development allows avoiding the use of the temperature-displacement analogy which overestimates the hygroscopic internal stress.

2. Materials and methods

2.1. Materials and manufacturing process

This study is devoted to the study of the hygroscopic behaviour of a unidirectional (UD) flax fibre-reinforced epoxy composite. The UD flax fibres are commercialised by Lineo Company under the commercial name FlaxTape™ 200. They present an aerial weight of $200\ g/m^2$ and a mass density of $1450\ kg/m^3$.

The epoxy resin is the SR8100 and was provided with its associated hardener SD 8823 by Sicomin. The mass ratio between the hardener and the resin is 26:100 g. Several flax-epoxy composite plates composed of six layers of UD flax fibres were prepared by the vacuum infusion process as shown in Figure 1. The vacuum pressure used in the manufacturing process was fixed to 0.7 bar. The infused plates were first cured for 24 hours at room

temperature and then polymerised at 60°C and 10% of RH in a climate chamber for 24 hours as recommended by the purveyor.

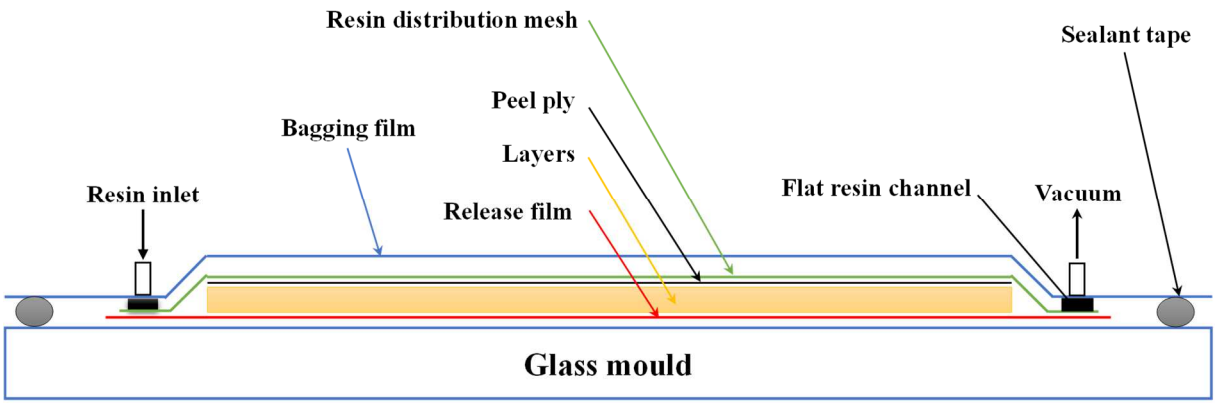

***Figure 1** . Schematic of the vacuum infusion process.*

2.2. Conditioning of the flax-epoxy samples

The flax-epoxy composite plates were cut to obtain square samples with 25 mm side length. These samples were then polished to have planar and even surfaces. All samples were dried at 60 °C for five days to remove any trace of water.

The thickness and mass of the flax-epoxy samples were measured in the dry state and are equal to 2.68 ± 0.10 mm and 1.99 ±0.10 g respectively. Their fibre volume fraction and their porosity rate are equal to 33.05 ± 1.78% and 4.64 ± 1.76%, respectively.

The ageing of the square flax-epoxy samples consisted in totally immersing them in tap water at room temperature until saturation. As shown in Figure 2 some of the composite samples were sealed with a waterproof paint to force water diffusion along the principal directions *x*, *y* and *z* where *x* is the direction of flax fibres, *y* is the transverse (or width) direction and *z* is the thickness direction.

The main objective is to assess the principal water diffusion parameters D_x, D_y and D_z as well as the saturation mass gains M_x, M_y and M_z.

During the ageing tests, the flax-epoxy samples were regularly weighed using a ±1 mg precision balance. Before each mass measurement, each sample was dried with a dry wipe to remove water from its surfaces. The amount of water absorbed after an immersion time *t* was calculated with the following expression:

$$M_t(\%) = \frac{W_t - W_0}{W_0} \times 100 \qquad \textbf{(1)}$$

where W_0 is the mass of the dry sample and W_t is its mass at time *t*.

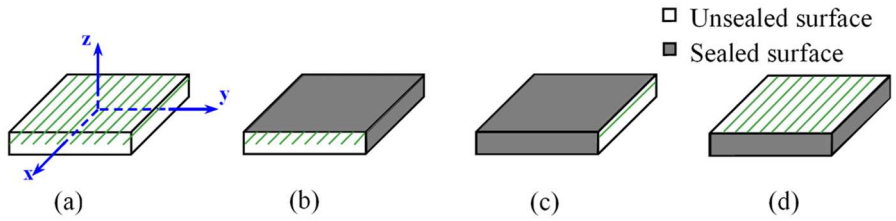

Figure 2. *Conditioning of the flax-epoxy samples: (a) unsealed and (b)-(d) sealed samples.*

2.3. Scanning electronic microscopy observations

Scanning electron microscopy (SEM) observations were performed on the flax-epoxy samples in the dry state and at saturation using a "JEOL JSM-7900F" scanning electron microscope operating at 1 kV. The flax-epoxy samples were cut and embedded in a thermoplastic resin and all the observed surfaces were polished using a double disc polishing machine. Before the microscopic observations, the flax-epoxy samples were dried in an oven at 40°C to remove water molecules and facilitate SEM observations.

2.4. Fick's analytical model

Several research works have shown that moisture uptake curves of natural fibre-reinforced polymer composites generally exhibit Fickian behaviour [1,8,19,26,30,38]. Fick's law is described by the following differential equation which allows to predict water diffusion as a function of time and space [20]:

$$\frac{\partial c}{\partial t} = \mathrm{div}(D.\nabla c) \tag{2}$$

where c is the moisture concentration and D is the diffusion tensor which is supposed symmetric in this work.

In our case, x, y and z are the principal directions and Fick's law can be rewritten as follows if water diffusion parameters are supposed constant:

$$\frac{\partial c}{\partial t} = D_x \frac{\partial^2 c}{\partial x^2} + D_y \frac{\partial^2 c}{\partial y^2} + D_z \frac{\partial^2 c}{\partial z^2} \tag{3}$$

The solution of Equation (3) reads [48,49]:

$$\frac{M_t}{M_\infty} = 1 - \left(\frac{8}{\pi^2}\right)^3 \sum_{i=0}^{\infty}\sum_{j=0}^{\infty}\sum_{k=0}^{\infty} \frac{\exp\left(-\pi^2 t\left(D_x\left(\frac{2i+1}{L}\right)^2 + D_y\left(\frac{2j+1}{L}\right)^2 + D_z\left(\frac{2k+1}{h}\right)^2\right)\right)}{\left((2i+1)(2j+1)(2k+1)\right)^2} \tag{4}$$

where M_t is the mass gain at time *t*, M_∞ is the saturation mass, and *L* and *h* are the flax-epoxy sample side and thickness.

In the case of sealed samples, water diffusion mainly occurs perpendicularly to the unsealed faces. Accordingly, the solution of Equation (3) reads for the three principal directions:

$$\frac{M_t}{M_\infty} = 1 - \left(\frac{8}{\pi^2}\right) \sum_{i=0}^{\infty} \frac{\exp\left(-\pi^2 t D_l \left(\frac{2i+1}{l}\right)^2\right)}{\left((2i+1)\right)^2} \quad \textbf{(5)}$$

where $D_l = D_x, D_y, D_z$ and $l = L,\ h$.

In order to determine the water diffusion parameters of the sealed and unsealed flax-epoxy samples, an optimisation algorithm was developed using the fminsearch function of Matlab. This program allows minimising the quadratic error q between the analytical solution of Fick's model and the experimental points:

$$q = \sum_{i=1}^{n} \left(M_a(t_k) - M_{\exp}(t_k)\right)^2 \quad \textbf{(6)}$$

where $M_a(t_k)$ is the moisture rate at time t_k evaluated from the analytical solution of Fick's model (Equations (4) and (5)) and $M_{\exp}(t_k)$ the experimental moisture content at time t_k.

3. Finite element analysis

In this section, the geometric plane modelling of flax-epoxy samples is firstly presented before developing the hygroscopic and hygroelastic finite element approximations. To account for their heterogeneity, three plane geometric models of the flax-epoxy specimens are considered in which the UD flax fibres and the epoxy matrix are modelled separately as described in section 3.1.

3.1. Description of the plane modelling

To simplify, a plane modelling of water diffusion in the flax-epoxy samples is considered as depicted in Figure 3. To model water diffusion along the direction of flax fibres and the thickness direction, three plane models are considered as depicted in Figure 3b, 3c and 3d. It is worthy to recall that the flax-epoxy samples are composed of six layers of UD flax fibres which explains the geometric models adopted in Figure 3b and 3d. Owing to symmetry, only a quarter of each plane surface is modelled as shown in Figure 3.

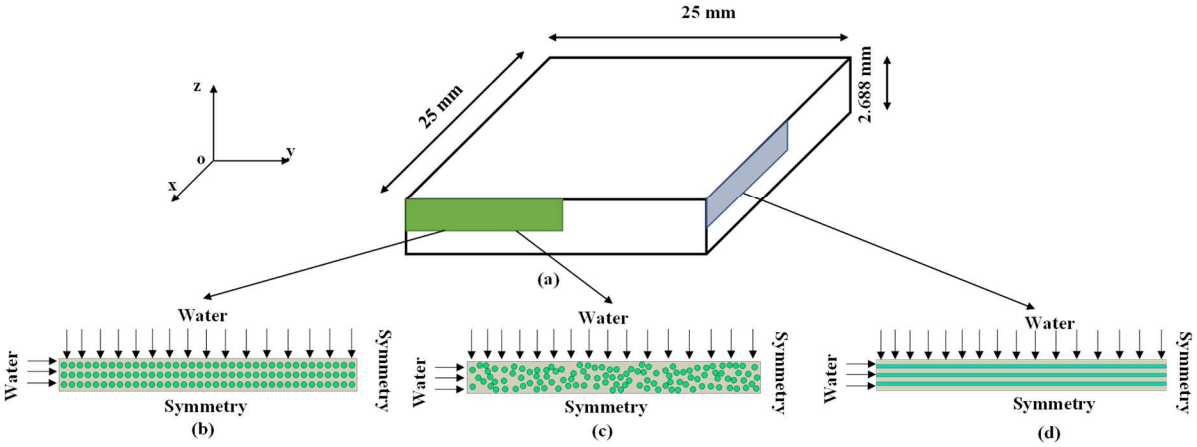

Figure 3. *(a) A square flax-epoxy specimen. (b)–(c) Plane modelling of water diffusion in the yz plane using (b) regular and (c) random distributions of flax fibres. (d) Plane modelling of water diffusion in the xz plane.*

Besides, the UD flax fibres bundles are supposed to present a circular cross section with diameter of $250\ \mu m$ and their number and distribution were chosen so as to respect the fibre volume fraction of the flax-epoxy composite ($V_f = 33.05\%$).

3.2. Hygroscopic and hygroelastic finite element approximations

To model the hygroscopic behaviour of the aged flax-epoxy specimens, the three-node hygroscopic membrane finite element developed by Zouari et al. [40] is considered.

For a 2D composite domain B_0 subjected to moisture boundary conditions applied at S_c as shown in Figure 4a, the weak form of Fick's differential equation reads:

$$w_1(c,c^*) = \int_{B_0} (\dot{c} - div(D \cdot \nabla c)) c^* dV = 0 \qquad \forall c^* \text{ with } \dot{c} = \frac{\partial c}{\partial t} \tag{7}$$

where c^* is a test function that verifies $c^* = 0$ on S_c

The weak form of Fick's diffusion equation can be rewritten as:

$$w_1(c,c^*) = \int_{B_0} \dot{c} c^* dV + \int_{B_0} \nabla c^* \cdot D \cdot \nabla c dV + \int_{\partial B_0} c^* \phi_n dV = 0 \qquad \forall c^* \tag{8}$$

where ϕ_n is the normal diffusion flux and ∂B_0 is the boundary of the 2D composite domain B_0

.

In the following, the formulation of the hygroscopic triangular element developed by Zouari et al. [40] is extended to the hygroelastic problem. The main objective is to predict the

mechanical stress that appears in the flax-epoxy samples when they are subjected to water ageing. To simplify, an uncoupled hygroelastic model is used and the term "uncoupled" is employed here to indicate that the mechanical variables have no influence on the hygroscopic parameters.

In addition to the hygroscopic equilibrium Equation (2), the quasi-static mechanical equilibrium is considered which, in the absence of body force, is written locally for a plane composite solid B_0 as:

$$\begin{cases} \sigma_{xx,x}(x,t)+\tau_{xy,y}(x,t)=0 \\ \tau_{xy,x}(x,t)+\sigma_{yy,y}(x,t)=0 \end{cases} \forall x \in B_0 \qquad \textbf{(9)}$$

where σ_{xx}, σ_{yy} and τ_{xy} are the plane components of the mechanical stress tensor ($\sigma_{xx,x} = \frac{\partial \sigma_{xx}}{\partial x}$).

The weak form of the static mechanical equilibrium Equation (9) is obtained by introducing a test function u^* that verifies $u^* = 0$ on S_u the part of ∂B_0 on which displacement boundary conditions are applied:

$$w_2(u,u^*) = \int_{B_0} \varepsilon^* \cdot \sigma \, dV - \int_{\partial B_0} u^* \cdot T \, dS = 0 \qquad \forall u^* \qquad \textbf{(10)}$$

where σ is the vector of plane stresses, ε^* is the vector of virtual plane strains and T is the vector of external surface forces applied on ∂B_0. It is worthy to note that a vectorial notation of the stress and strain tensors is used in Equation (10) instead of tensorial notation to simplify the construction of the finite element approximation.

The stress vector σ can be written in the following form:

$$\sigma = H \cdot \varepsilon^{el} \rightarrow \sigma = H \cdot (\varepsilon - \varepsilon^h) \qquad \textbf{(11)}$$

where H is the elasticity matrix and ε^h is the vector of hygroscopic strains induced by moisture diffusion within the flax-epoxy samples. This vector is written as a function of the moisture content $c(x,t)$ using the following linear expression:

$$\varepsilon^h(x,t) = \beta^h(x,t) c(x,t) \qquad \textbf{(12)}$$

where β^h is the hygroscopic expansion vector which is considered independent of the ageing time in this study.

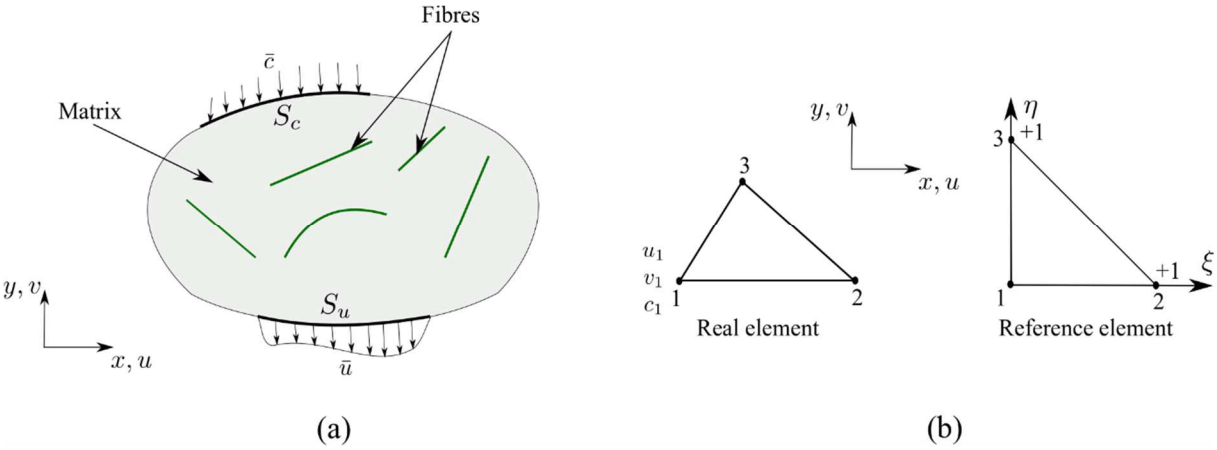

Figure 4 . *(a) 2D composite solid with moisture and displacement boundary conditions. (b) The three-node hygroelastic membrane finite element.*

By combining Equations (8) and (10), the weak form of the hygroelastic equilibrium of the composite medium B_0 is obtained:

$$w(c,c^*,u,u^*)=\int_{B_0}\dot{c}\,c^*dV+\int_{B_0}\nabla c^*\cdot D\cdot\nabla c dV+\int_{\partial B_0}c^*\phi_n dS+\int_{B_0}\varepsilon^*\sigma dV-\int_{\partial B_0}u^*T dS=0\quad\forall\,u^*,c^* \tag{13}$$

The resolution of the weak form (13) requires spatial and time discretization. For the spatial discretization, the triangular hygroscopic membrane element of Zouari et al. [40] is considered and displacement degrees of freedom are added to estimate the mechanical strains. The three-node triangular hygroelastic element is shown in Figure 4b. The three shape functions associated with the three-node triangular membrane element allow us to approximate the displacements along *x* and *y*, denoted *u* and *v*, as well as the moisture concentration:

$$u=\sum_{i=1}^{3}N_i(\zeta,\eta)u_i\ ;\ v=\sum_{i=1}^{3}N_i(\zeta,\eta)v_i\ ;\ c=\sum_{i=1}^{3}N_i(\zeta,\eta)c_i \tag{14}$$

By using the approximations (14), it is possible to show that $_c$, ∇c , $_u$ and $_\varepsilon$ are related to $u_n=\{\cdots u_i\ v_i\ c_i\cdots\ i=1,3\}^t$, the nodal degrees of freedom vector of the hygroelastic element, as follows:

$$c={}^tN_c\cdot u_n\ ;\ u=N_u\cdot u_n\ ;\ \nabla c=B_c\cdot u_n\ ;\ \varepsilon=B_m\cdot u_n \tag{15}$$

At the element level, the finite element approximation of the weak form (13) is written:

$$w^e(u_n^*, u_n) = {}^t u_n^* \cdot \left[\int_{B_0} N_c \, {}^t N_c dV \cdot \ddot{u}_n + \left(\int_{B_0} {}^t B_c \, D \, B_c dV + \int_{B_0} {}^t B_m \, H \, B_m dV - \int_{B_0} {}^t B_m \, H \, \beta_m \, {}^t N_c dV \right) u_n + \int_{Sc} N_c \, \phi_n dS - \int_{Sc} N_u \, T dS \right]$$

$$\forall u_n^* \quad \textbf{(16)}$$

After simplification, the finite element equation is written at the elementary level:

$$K_{eq} \cdot u_n + C \cdot \ddot{u}_n - F_{eq} = 0 \qquad \textbf{(17)}$$

where $C = \int_{B_0} N_c \, {}^t N_c dV$, $F_{eq} = \int_{Sc} N_c \, \phi_n dS - \int_{Sc} N_u \, T dS$ and $K_{eq} = K_c + K_m - K_{mc}$ with

$K_c = \int_{B_0} {}^t B_c \, D \, B_c dV$, $K_m = \int_{B_0} {}^t B_m \, H \, B_m dV$ and $K_{mc} = \int_{B_0} {}^t B_m \, H \, \beta_m \, {}^t N_c dV$.

For the time integration of Equation (17), the loading interval $[t, t+\Delta t]$ is considered. The backward Euler integration of Equation (17) gives the elementary residual vector at $t+\Delta t$:

$$R^{t+\Delta t} = K_{eq} \cdot u_n^{\,t+\Delta t} + C \cdot \frac{\Delta u_n}{\Delta t} - F_{eq}^{\,t+\Delta t} \text{ with } \Delta u_n = u_n^{\,t+\Delta t} - u_n^{\,t} \qquad \textbf{(18)}$$

The elementary tangent stiffness matrix $K_T^{\,t+\Delta t}$ of the three-node hygroelastic membrane element is obtained by differentiating the residual vector $R^{t+\Delta t}$ with respect to Δu_n :

$$K_T^{\,t+\Delta t} = -\frac{\partial R^{t+\Delta t}}{\partial \Delta u} = -K_{eq} - \frac{C}{\Delta t} \qquad \textbf{(19)}$$

The triangular hygroelastic finite element has been implemented in the commercial finite element code ABAQUS using a user element subroutine.

4. Results and discussion

4.1. Water diffusion parameters of the sealed samples

In this part, the water diffusion parameters of the sealed flax-epoxy samples are identified using the optimisation procedure described in section 2.4. Figure 5 shows the water uptake curves of the sealed flax-epoxy samples and Table 1 summarises their principal water diffusion parameters identified from the optimisation procedure.

In fact, D_x is found 100 times larger than D_z and approximately 2.3 times greater than D_y . This difference is related to the composition of the flax fibre which promotes water transport along its stem particularly through the lumen [31,50–52]. In fact, the hydrophilic components

of the flax fibre (cellulose, hemicellulose and pectin) promote water diffusion along its longitudinal direction [4,8,30,53].

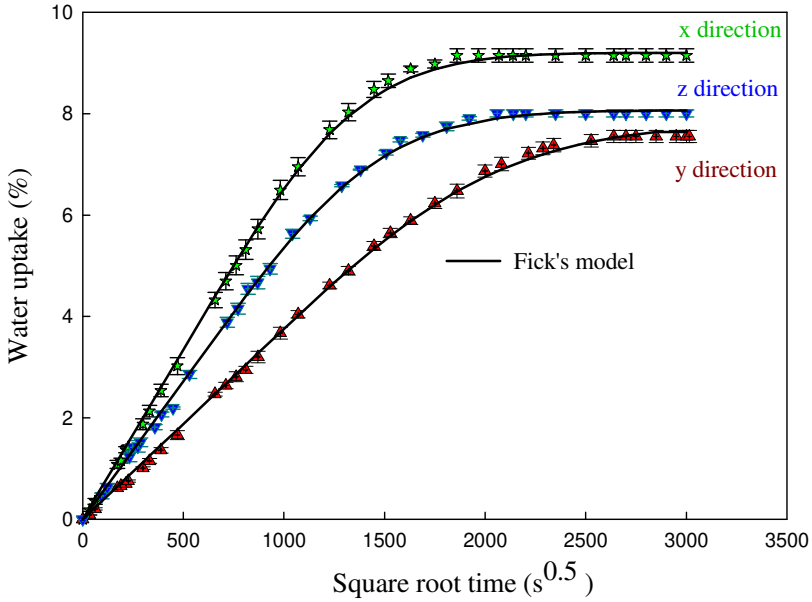

Figure 5 . *Experimental water uptake curves of the sealed flax-epoxy samples compared with 1D Fick's model solution.*

Table 1 : Water diffusion parameters of the sealed flax-epoxy sample.

D_x	D_y	D_z	Weight gains at saturation $M_\infty(\%)$			$R_x = \frac{D_x}{D_z}$	$R_y = \frac{1}{1}$
$(10^{-7}\, mm^2/s)$	$(10^{-7}\, mm^2/s)$	$(10^{-7}\, mm^2/s)$	$M_\infty^x(\%)$	$M_\infty^y(\%)$	$M_\infty^z(\%)$		
648.65± 0.64	285.79±0.01	6.45±0.01	9.14±0.13	7.55±0.12	8.01±0.07	100.56	44.30

Besides, the weight gain at saturation in the direction of the flax fibres is found greater than those in the transverse and thickness directions. Indeed, this could be explained by the increase of diffusion rate (defined as the slope of the absorption curve) which further promotes the swelling of flax fibres and leads to more matrix swelling and propagation of micro-cracks at the fibre-matrix interface. This process further weakens the aged flax-epoxy samples and thus increases their water absorption capacity. These explanations are supported by the SEM observations of Figure 6 on sealed flax-epoxy samples at saturation.

In particular, Figure 6a shows micro-cracks at the fibre-matrix interface which can be induced by the formation of hydrogen bonds between the hydrophilic components of the flax fibre primary wall (pectin, hemicellulose) and water molecules [54]. Figure 6b shows micro-cracks in the bundle of flax fibres mainly caused by the differential hygroscopic swelling between the fibre-fibre and fibre-matrix interfaces. The presence of these micro-cracks increases by capillarity water diffusion in these composite samples. Figure 6c shows the formation of

micro-porosities with an average size of 0.2 µm which is smaller than the lumen size (D_{lumen} = 5-10 µm) [55].

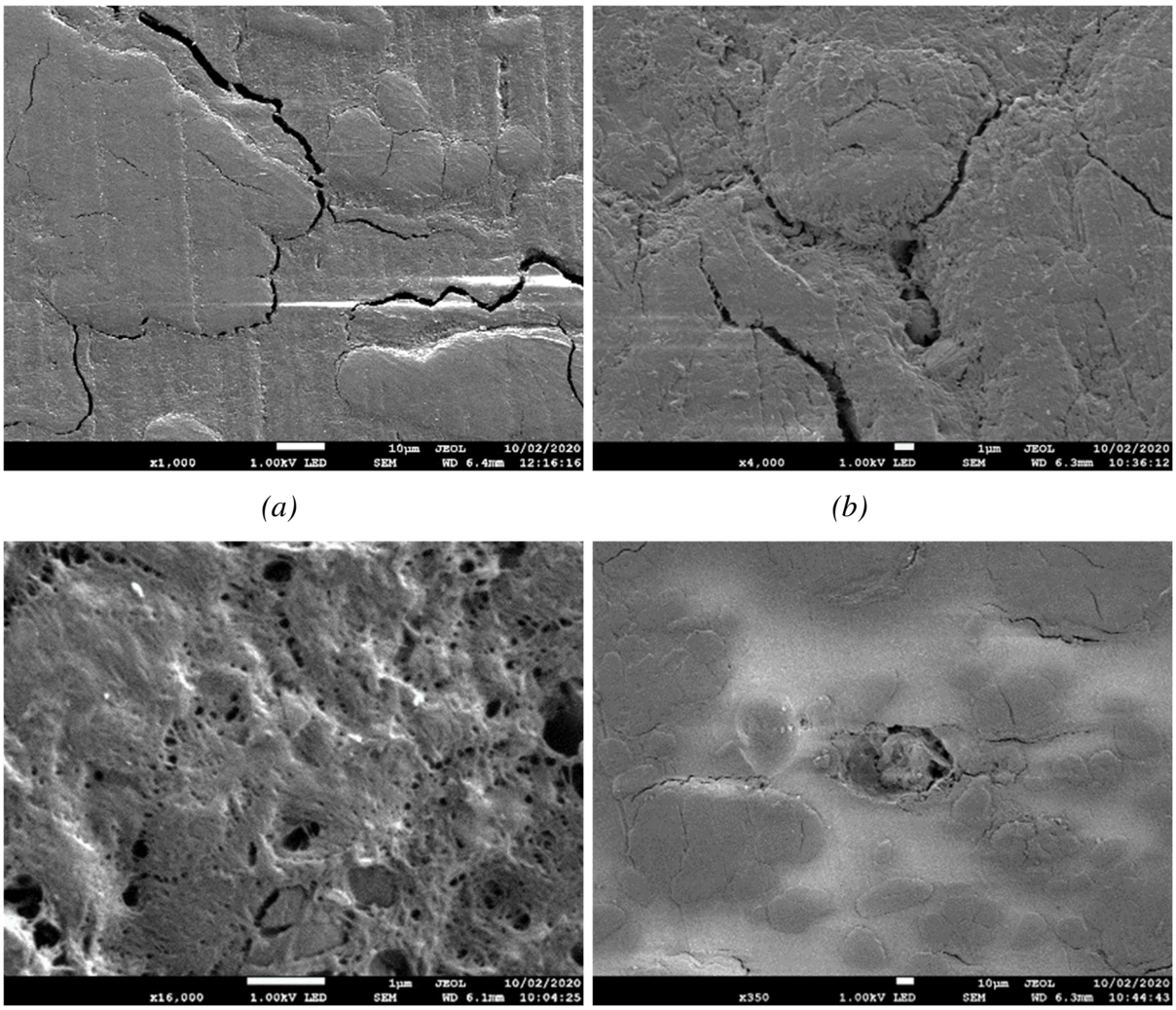

(a) *(b)*

(c) *(d)*

Figure 6 . *SEM micrographs of cross sections of 60-day aged flax-epoxy samples with water diffusion in the direction of flax fibres.*

This can be explained by the dissolution in water of some flax fibre components such as pectins. These voids increase the weight gain at saturation of the flax-epoxy samples. Figure 6d shows a partial pull-out of a flax fibre and this can be explained by a possible failure due to the differential hygroscopic swelling of the flax fibres.

For water diffusion along the transverse and thickness directions (*y* and *z* directions), the weight gain at saturation M_{∞}^{y} is found lower than M_{∞}^{z} while D_{y} is 44.30 times D_{z} (Table 1). These variations are mainly related to the sample's dimensions where the width (*y* direction) is almost 10 times the thickness (*z* direction). In fact, when the dimensions increase the weight gain at saturation decrease and the water diffusion coefficients increase. The

decrease of the saturation weight with sample dimensions has been also reported in the case of other composite materials and some explanations have been proposed [30,31,56]. Bunsell et al. [56] have attributed this variation to a molecular rearrangement of the polymeric network when samples are thicker which would slow down the water diffusion in the composite. For the flax-epoxy samples studied in this work, the variation of the saturation weight with the dimensions could also be accentuated by the increase of moisture diffusion kinetics, which causes more swelling of the flax fibres and the epoxy matrix as previously explained.

4.2. 3D water diffusion parameters of the flax-epoxy specimens

Most of the moisture diffusion analyses of the literature show that water diffusion in bio-composites is complex and the diffusion parameters identified from the sealed samples do not allow describing the 3D water diffusion behaviour. This is also confirmed by Figure 7a which represents a comparison between the experimental water uptake curve of the unsealed flax-epoxy samples and the 3D Fick's model solution obtained with water diffusion parameters of the sealed specimens (Table 1).

Accordingly, the principal water diffusion parameters D_x, D_y and D_z of the unsealed flax-epoxy samples should be identified at the same time by the optimization procedure with two additional constraints on the principal diffusion parameters: $D_y < D_x$ and $D_z < D_y$. These two constraints are deduced from the identification of water diffusion parameters of the sealed flax-epoxy samples (Table 1).

To this end, a penalty function is added to the quadratic error q and the new objective function is written as follows:

$$f_{obj} = q + \rho \max(0, D_x - D_y, D_y - D_z) \quad \textbf{(20)}$$

where ρ is a penalty factor.

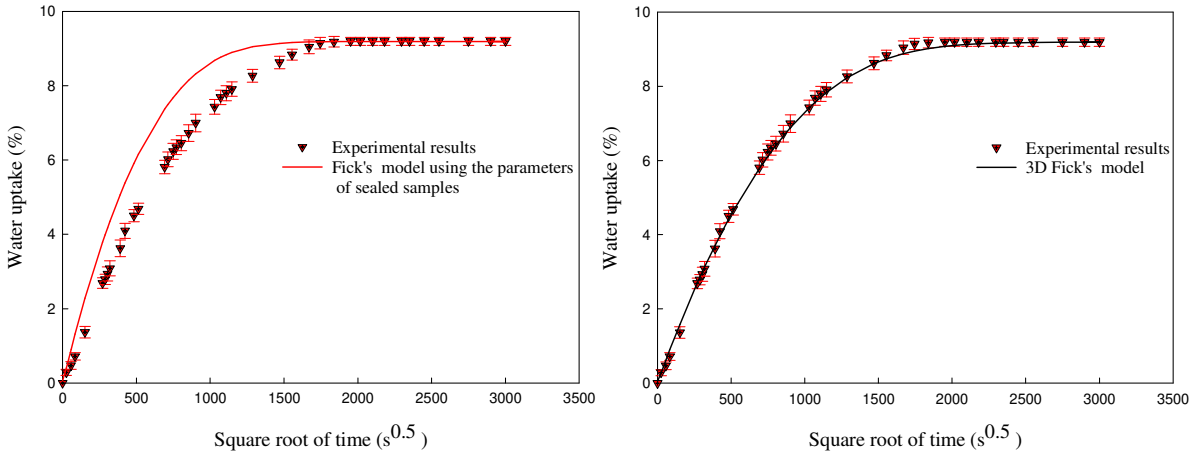

(a) *(b)*

Figure 7. *Experimental water uptake curve of the unsealed flax-epoxy samples compared with 3D Fick's model solution obtained with: (a) the diffusion parameters of the sealed samples (red curve) (b) the diffusion parameters of Table 2 (black curve).*

Table 2 : Water diffusion parameters of the unsealed flax-epoxy samples

D_x $(10^{-7}\,mm^2/s)$	D_y $(10^{-7}\,mm^2/s)$	D_z $(10^{-7}\,mm^2/s)$	$M_\infty^x(\%)$	$R_x=\frac{D_x}{D_z}$	$R_y=\frac{D_y}{D_z}$
213.09±0.01	107.38±0.08	3.55±0.01	9.15± 0,10	60,00	30,22

Table 2 summarises the identified water diffusion coefficients of the unsealed flax-epoxy samples and Figure 7b shows that these optimal parameters allow correctly describing the hygroscopic behaviour of these samples.

It is interesting to note that the water diffusion parameters of the unsealed flax-epoxy specimens (Table 2) are different from those of the sealed samples (Table 1).

Besides, the ratios R_x and R_y of the unsealed samples show a decrease by 41% and 32% respectively compared with those of the sealed samples (Table 1). This decrease is probably related to the movement of water particles which are forced to follow one of the three main directions in the case of sealed samples, in particular in the direction of flax fibres which explains the important value of R_x for sealed samples. For the unsealed specimens, the privileged direction is less pronounced than in the case of sealed samples, and a kind of hygroscopic balance between the three main directions is obtained, which could explain the relatively large decrease in R_x and R_y.

At the end of this study, by making the hypothesis that the moisture diffusion process is mainly controlled by the unidirectional flax fibres, a ratio between their longitudinal and radial water diffusion coefficients (denoted D_f^L and D_f^R) equivalent to that resulting from the optimization procedure on unsealed samples $(R_x = D_x / D_y = 60)$ can be deduced. This ratio is considered in section 4.3 to estimate the longitudinal and radial moisture diffusion coefficients of the flax fibre with the hypothesis $D_f^L = 60\ D_f^R$.

4.3. Finite element analysis of the hygroscopic behaviour

In this part, the hygroscopic behaviour of the flax-epoxy samples is modelled using the hygroscopic plane finite element of Zouari et al. [40] (three-node triangular membrane element with only moisture degrees of freedom). To this end, the water diffusion coefficients of the epoxy resin and those of the UD flax fibres are needed. The hygroscopic behaviour of the pure epoxy resin is supposed isotropic and characterised by the water diffusion coefficient

$D_m = 5.42\times10^{-7}\,\mathrm{mm^2/s}$ obtained from its experimental water uptake curve. This value is close to other epoxy moisture diffusion coefficients reported in the literature [57,58].

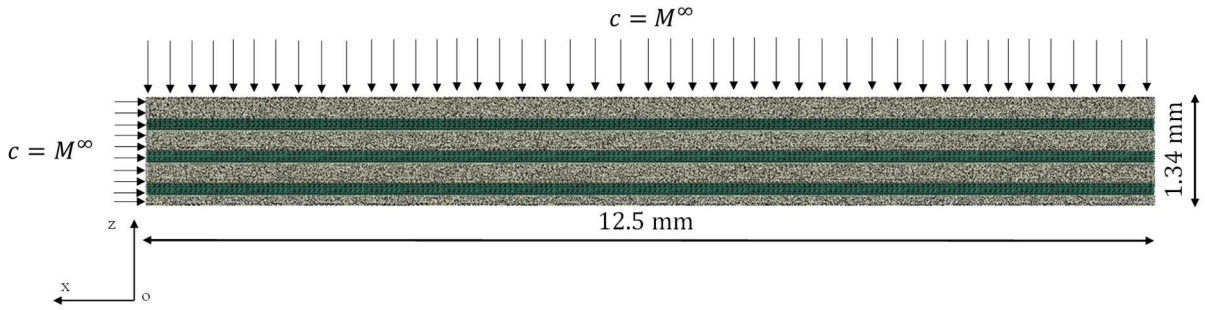

Figure 8 . *Finite element modelling of water diffusion in the unsealed flax-epoxy samples using 56,232 three-node hygroscopic elements.*

For the UD flax fibres, their water diffusion behaviour is anisotropic and should be principally described by a radial and a longitudinal coefficient denoted D_f^L and D_f^R [8,39,40,59,60].

Although some works in the literature have focused on the determination of the flax fibre radial diffusion coefficient as the work by Célino et al [61], the determination of its longitudinal diffusion parameter remains almost inexistent in the literature. Therefore, an estimation of the radial and longitudinal water diffusion parameters of the flax fibre is proposed in this section by considering an inverse approach. As explained at the end of section 4.2, a ratio of 60 between D_f^L and D_f^R is considered.

To begin, a first approximation of the radial diffusion coefficient of the flax fibre was obtained by means of Halpin-Tsai homogenisation model [62] knowing the value of D_m and the water diffusion parameter across the thickness of the sealed flax-epoxy samples $(D_z = 6.45\times10^{-7}\,\mathrm{mm^2/s})$. In this case, the first approximation of the radial diffusion parameter of the flax fibre is $D_f^R = 5.45\times10^{-7}\,\mathrm{mm^2/s}$. The water diffusion coefficients D_f^R, D_f^L $(D_f^L = 60D_f^R)$ and D_m are now used as inputs of the finite element model of Figure 3d to simulate water diffusion in the unsealed flax-epoxy specimens. It is worthy to note that the finite element modelling is conducted in the *xz* plane (Figure 3d) because it considers the radial and longitudinal diffusion coefficients of the UD flax fibres (D_f^L and D_f^R).

In fact, the modelling in the *yz* plane (Figure 3b) allows considering only the radial diffusion parameter of the flax fibre which could bias its estimation. It is also important to recall that the aged flax-epoxy samples are constituted of six layers of UD flax fibres, which leads to a

total thickness of 2.68 mm. Owing to symmetry, one-quarter of the *xz* plane is modelled as shown in Figure 8. The three layers of UD flax fibres are modelled in this plane by three rectangles of thickness 0.147 mm to respect the fibre volume fraction of 33%. The refined mesh of Figure 8 constituted of 56232 elements was fixed after a mesh convergence study. The moisture boundary conditions are applied to the top and left edges of the 2D finite element model ($c = M^{\infty} = 9.15\%$).

Figure 9 shows a comparison between the experimental and the numerical water uptake curves of the unsealed flax-epoxy samples using the first set of diffusion parameters (the red curve). It is worthy to note that the numerical water uptake curve was calculated as the arithmetic average of all nodal moisture concentrations of the finite element model. The obtained results indicate that the numerical curve does not accurately describe the experimental curve. The difference between these two curves reflects the difficulty of predicting the hygroscopic behaviour of the flax-epoxy samples using a heterogeneous model. In the following a better approximation of the radial and longitudinal water diffusion coefficients of the flax fibre is proposed to correctly fit the experimental curve of the unsealed flax-epoxy samples. To this end, D_m and D_f^R have been varied while always keeping $D_f^L = 60\, D_f^R$ until fitting the experimental curve (see Zouari et al. [40] for more details about this inverse procedure). Accordingly, the following optimal parameters $D_f^R = 16.32\times10^{-7}\,\mathrm{mm^2/s}$, $D_f^L = 979.21\times10^{-7}\,\mathrm{mm^2/s}$ and $D_m = 5.66\times10^{-7}\,\mathrm{mm^2/s}$, have been obtained and allow an accurate prediction of the experimental curve as shown in Figure 9 (the black curve).

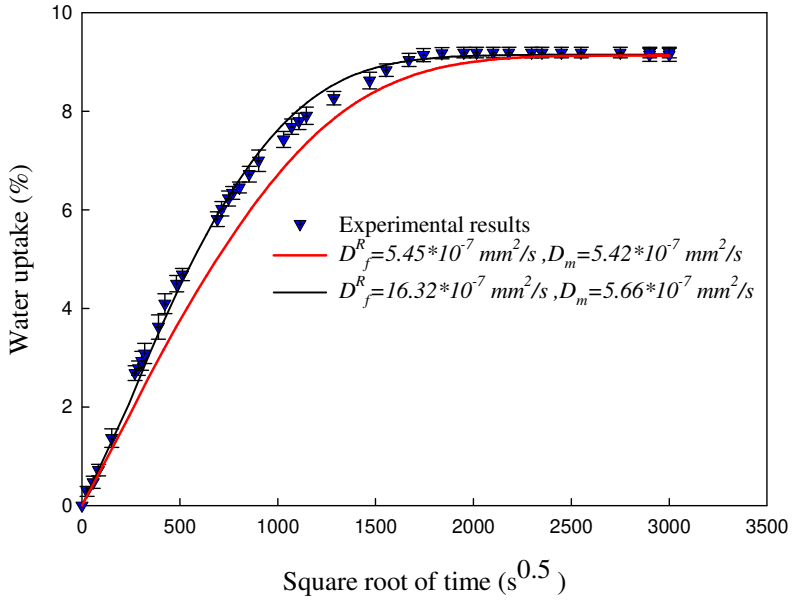

Figure 9. *Comparison between the experimental and the numerical water uptake curves of the unsealed flax-epoxy samples by considering the first set of parameters (red curve):* $D_f^R = 5.45\times10^{-7}\,\mathrm{mm^2/s}$ *and* $D_m = 5.42\times10^{-7}\,\mathrm{mm^2/s}$ *and the second set of parameters (black curve) :* $D_f^R = 16.32\times10^{-7}\,\mathrm{mm^2/s}$ *,and* $D_m = 5.66\times10^{-7}\,\mathrm{mm^2/s}$.

It is interesting to note that the water diffusion coefficient of the epoxy matrix in the flax-epoxy samples ($D_m = 5.66\times10^{-7}\,\mathrm{mm^2/s}$) is slightly greater than that of the pure epoxy resin ($D_m = 5.42\times10^{-7}\,\mathrm{mm^2/s}$).

This behaviour has been already reported in the case of synthetic fibre [43,63] and also natural fibre reinforced composites [39,40,43]. It can be explained firstly by the presence of porosities in the flax-epoxy samples, compared to the epoxy pure resin specimens, and secondly the appearance of micro-cracks due to the dissimilar swelling between the flax fibres, very hydrophilic, and the epoxy matrix, rather hydrophobic compared to the reinforcement. These defects can make the epoxy matrix more brittle to moisture diffusion and partly explains the increase in its water diffusion coefficient.

Concerning the longitudinal and radial moisture diffusion coefficients of the flax fibre ($D_f^R = 16.32\times10^{-7}\,\mathrm{mm^2/s}$ and $D_f^L = 979.21\times10^{-7}\,\mathrm{mm^2/s}$), they seem in good agreement with some experimental results of the literature [61,64]. For example, Stamboulis et al. [64] have reported a value of the flax fibre diffusion parameter equal to $1\times10^{-4}\,\mathrm{mm^2/s}$ for a flax fibre bundle of 1.5 mm of length aged at 100% of relative humidity at room temperature. This value of D_f^L is very close to that estimated in this work. In another work, Célino et al. [61] have studied moisture diffusion kinetics in UD flax samples aged by total immersion in water at room temperature. They have assumed that moisture diffusion principally occurs across the radial direction of the flax fibres and have reported a radial diffusion parameter of $11.9\times10^{-7}\,\mathrm{mm^2/s}$ which is also close to the value estimated in this study.

4.4. Finite element analysis of the hygroelastic behaviour

In this section, the three-node triangular hygroelastic finite element presented in section 3.2 is considered to estimate the internal hygroscopic stress that appears in the aged flax-epoxy samples. To this end, the finite element model of Figure 10a with displacement and moisture boundary conditions is considered. It is worthy to note that this modelling is conducted in the *yz* plane where the sections of the UD flax fibres are modelled in a first approximation with circles of diameter 0.25 mm.

The main objective is to more accurately estimate the hygroscopic stress caused by water ageing compared to a modelling in the *xz* plane (Figure 3b and 3c). The influence of the distribution of the UD flax fibres in the flax-epoxy samples is also studied by considering the random distributions of Figure 10b, 10c and 10d in addition to the regular distribution of Figure 10a.

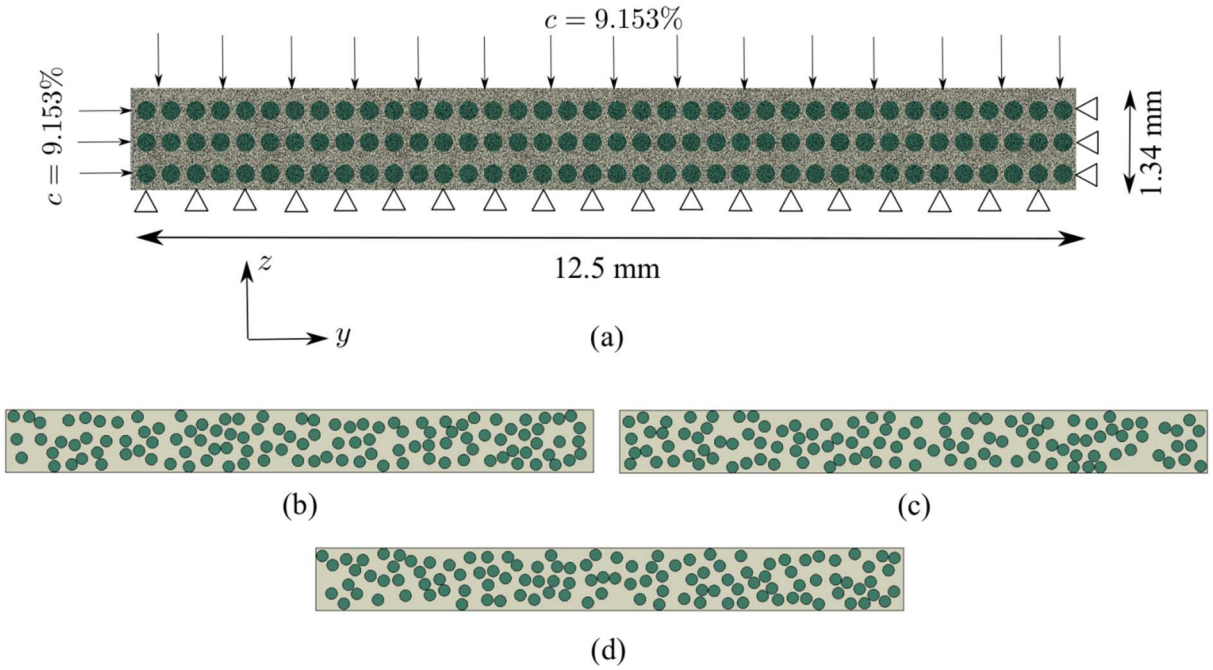

Figure 10. *(a) Plane finite element modelling of the hygroelastic behaviour of the unsealed flax-epoxy samples with a mesh of 78,452 triangular elements. (b)-(d) Plane modelling with three random distributions of the flax fibres.*

For the hygroscopic and elastic material properties of the epoxy matrix and the UD flax fibres to be used with the finite element models of Figure 10, the water diffusion parameters estimated in section 4.3 in relation with the unsealed flax-epoxy samples ($D_m = 5.66\times10^{-7}\,\text{mm}^2/\text{s}$ and $D_f^R = 16.32\times10^{-7}\,\text{mm}^2/\text{s}$) are firstly considered. For the hygroscopic expansion coefficients, the following epoxy matrix coefficient $\beta_m = 0.24$ is used and constitutes an average of some coefficients reported in the literature [65–68]. In addition, the hygroscopic expansion of the epoxy matrix is assumed to be isotropic. For the UD flax fibres, their radial hygroscopic expansion coefficient is particularly considered based on the plane models of Figure 10.

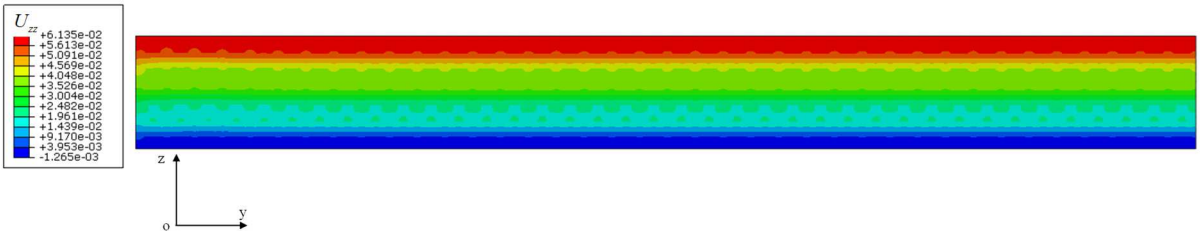

Figure 11. *Distribution of the transverse displacement at saturation (after 66 days of immersion) of the unsealed flax-epoxy samples modelled with a regular distribution of the flax fibres.*

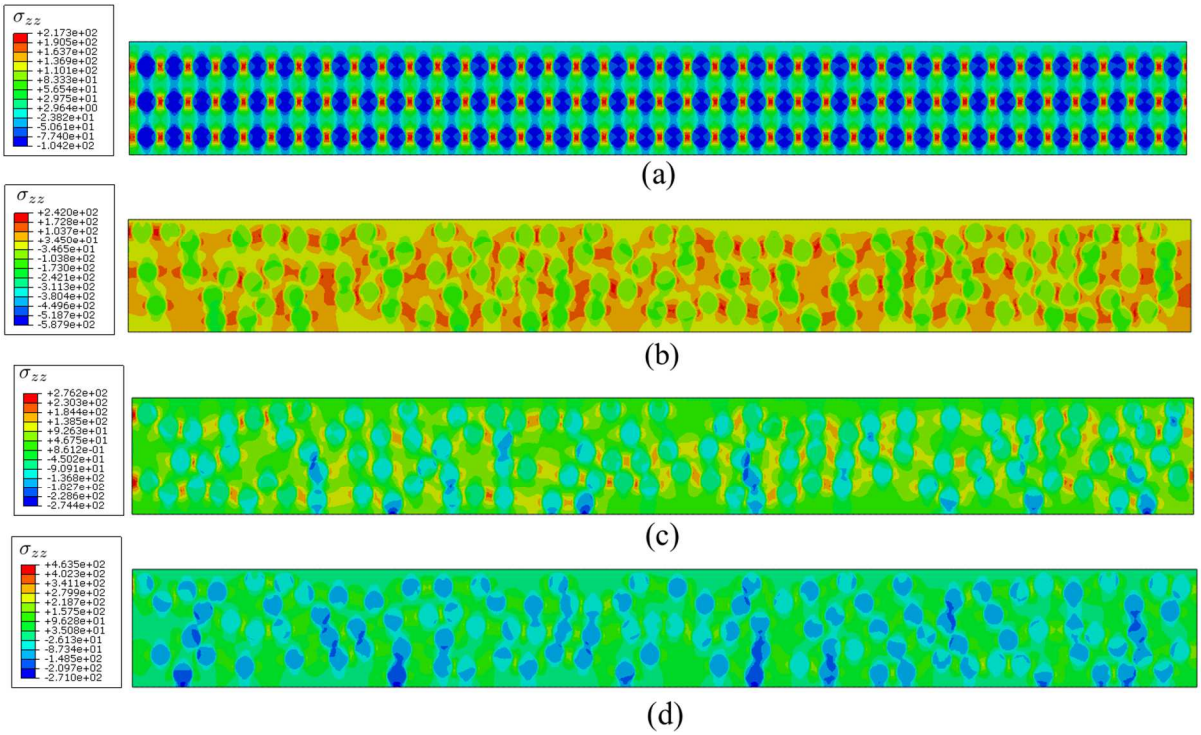

Figure 12. *Distribution of the internal stress across the thickness σ_{zz} inside the unsealed flax-epoxy samples after 66 days of immersion: (a) regular distribution of the flax fibres, (b)-(d) random distributions of the flax fibres.*

To this end, the radial expansion coefficient reported by Péron et al. [69] ($\beta_f^R = 0.97$) is used which seems to be in agreement with that given by Le Duigou et al. [70] ($\beta_f^R = 1.14$) and the expansion parameter reported by Garat et al. [71] ($\beta_f^R = 1.07$). For the longitudinal hygroscopic expansion coefficient of the UD flax fibres, Le Duigou et al. [72] have explained that it is very negligible with respect to β_f^R and close to zero as for wood fibres.

Figure 12 shows the distribution of the hygroscopic internal stress across to the thickness (σ_{zz}) at saturation within the aged flax-epoxy samples using regular and random distributions

of the flax fibres. It is important to note that the phenomenon of hygroscopic swelling mainly occurs across to the thickness of the aged samples which explains the particular study of σ_{zz}. Figure 13 also shows the evolution of the mean transverse stress during ageing in the matrix (Figure 13a), in the reinforcement (Figure 13b) and in the composite sample (Figure 13c). These results show that, overall, the flax fibres are subjected to hygroscopic compression stress while the epoxy matrix is subjected to tensile stress. The compression stress that appears in the reinforcement can be explained by the fact that the flax fibres and the epoxy matrix don't swell in the same way, although they present the same moisture concentration at saturation $(c=9.153\%)$. This is due to the difference between their hygroscopic swelling parameters ($\beta_f^R \approx 4\beta_m$). Thus, the flax fibres have tendency to swell more than the epoxy matrix and are therefore found constrained by the latter. In addition, it is worth noting that the flax fibres distribution can significantly influence the transverse internal stress distribution within the flax-epoxy sample as shown in Figure 12. Indeed, the stress peaks, which are mainly localized in the epoxy matrix, vary from 217.3 MPa (regular distribution) to 463.5 MPa found with the third random finite element model (Figure 12d). Similar stress peaks have been already reported in the case of synthetic fibre-reinforced polymer composites where the synthetic fibres have been supposed hydrophobic (moisture diffusion and hygroscopic expansion parameters equal to zero) [41,46]. In the work by Ouled Ahmed et al. [46], stress peaks close to 300 MPa within glass-polyester composites aged in distilled water have been found.

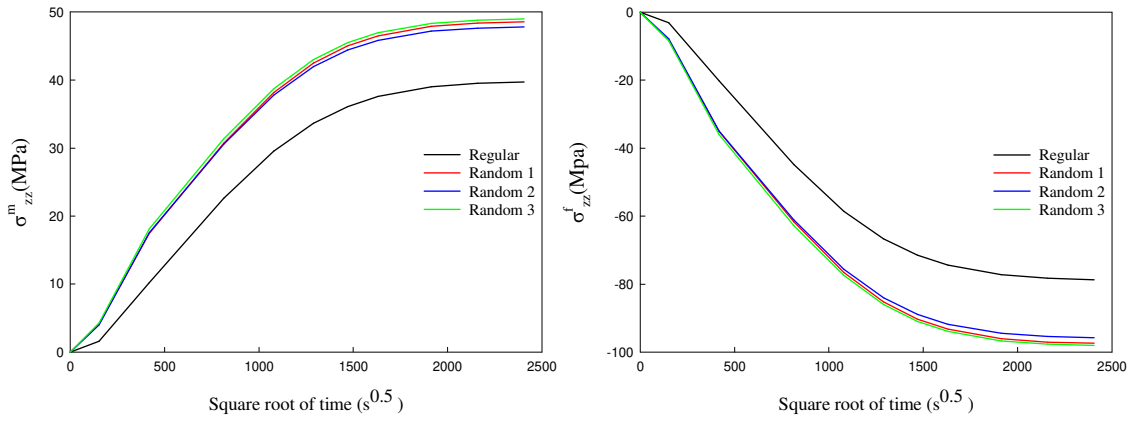

(a) (b)

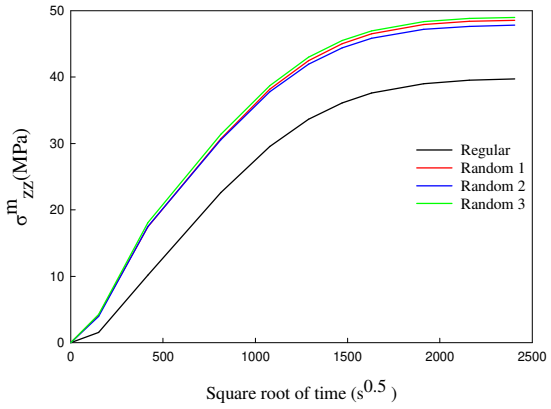

(c)

Figure 13 *. Evolution of the transverse mean stress during ageing inside: (a) the matrix* $\overline{\sigma}^{m}_{zz}$*, (b) the reinforcement* $\overline{\sigma}^{f}_{zz}$ *and (c) the flax-epoxy composite sample.*

The relatively high levels of internal stress found in this study, which are certainly overestimated by the current uncoupled hygroelastic model, exceed in particular the tensile strength of the epoxy matrix (around 40 MPa), which can lead to the initiation of damage by matrix cracking, delamination and degradation of the flax fibres without adding external loads.

This could explain the micro-cracks in the matrix close to the fibre-matrix interface depicted in Figure 6a as well as cracks in the flax fibre bundle shown in Figure 6b. Despite the high difference in the transverse internal stress distribution between the regular and random finite element models, the mean value of this hygroscopic stress varies from 40 to 50 MPa in the matrix and from 80 to 100 MPa in the reinforcement (Figure 13)

5. Conclusion

In this paper, the transient hygroscopic behaviour of unidirectional (UD) flax fibre-reinforced epoxy composite aged by immersion in tap water at room temperature until saturation was firstly investigated. To this end, the absorption water uptake curves of sealed and unsealed flax-epoxy samples, which present Fickian behaviour, allowed identifying their macroscopic water diffusion parameters using an optimisation approach. The main conclusion drawn from this first part is that water diffusion is much more predominant in the direction of the flax fibres than the thickness and the width directions. Secondly, the results of the first part were considered to estimate the flax fibre radial and longitudinal water diffusion parameters using a numerical inverse procedure. This was conducted by a plane finite element model that takes into account the heterogeneity of the flax-epoxy samples. The obtained flax fibre diffusion

parameters seem in good accordance with other literature results. Finally, the estimation of the hygroscopic internal stress that appears in the flax-epoxy samples due to water ageing was investigated. To this end, a three-node triangular membrane finite element based on an uncoupled hygroelastic model was developed. Finite element simulations with regular and random distributions of the flax fibres were conducted and important stress peaks were obtained particularly in the matrix domain. These stress levels exceed in particular the tensile strength of the epoxy matrix (around 40 MPa), which can lead to the initiation of damage inside the flax-epoxy samples without external loads.

As a future work, it would be interesting to consider another hygroscopic model to describe water diffusion kinetics within the aged samples. In fact, Fick's model used in this study can't take into account the maximum amount of water absorbed by the epoxy matrix since it makes the assumption that water molecules move freely within the aged composite samples. This is in contradiction with the water uptake curve of the pure epoxy resin showing a maximum water uptake of 1.1% while the moisture boundary conditions applied to the finite element models of this study largely exceed this value (~ 10%). This may partly explain the overestimation of the internal hygroscopic stress in the matrix found by the hygroelastic finite element modelling. To this end, the use of a more general diffusion model like that of Langmuir could be considered. In addition to the hygroscopic model, the use of a fully coupled hygroelastic model between the mechanical and the hygroscopic variables leads to a more accurate estimation of the hygroscopic stress inside the flax-epoxy specimens.

References

[1] Abd El-baky M, Attia M. Water absorption effect on the in-plane shear properties of jute–glass–carbon-reinforced composites using Iosipescu test. Journal of Composite Materials 2019;53:3033–45. https://doi.org/10.1177/0021998318809525.

[2] Pickering KL, Efendy MGA, Le TM. A review of recent developments in natural fibre composites and their mechanical performance. Composites Part A: Applied Science and Manufacturing 2016;83:98–112. https://doi.org/10.1016/j.compositesa.2015.08.038.

[3] George M, Chae M, Bressler DC. Composite materials with bast fibres: Structural, technical, and environmental properties. Progress in Materials Science 2016;83:1–23. https://doi.org/10.1016/j.pmatsci.2016.04.002.

[4] Célino A, Freour S, Jacquemin F, Casari P. The hygroscopic behavior of plant fibers: a review. Front Chem 2014;1. https://doi.org/10.3389/fchem.2013.00043.

[5] Al-Hajaj Z, Sarwar A, Zdero R, Bougherara H. In-situ damage assessment of a novel carbon/flax/epoxy hybrid composite under tensile and compressive loading. Journal of Composite Materials 2019;53:2701–14. https://doi.org/10.1177/0021998319839129.

[6] Moudood A, Rahman A, Khanlou HM, Hall W, Öchsner A, Francucci G. Environmental effects on the durability and the mechanical performance of flax fiber/bio-epoxy composites. Composites Part B: Engineering 2019;171:284–93. https://doi.org/10.1016/j.compositesb.2019.05.032.

[7] Sergi C, Tirillò J, Seghini MC, Sarasini F, Fiore V, Scalici T. Durability of Basalt/Hemp Hybrid Thermoplastic Composites. Polymers (Basel) 2019;11. https://doi.org/10.3390/polym11040603.

[8] Saidane EH, Scida D, Assarar M, Ayad R. Assessment of 3D moisture diffusion parameters on flax/epoxy composites. Composites Part A: Applied Science and Manufacturing 2016;80:53–60. https://doi.org/10.1016/j.compositesa.2015.10.008.

[9] Chilali A, Zouari W, Assarar M, Kebir H, Ayad R. Effect of water ageing on the load-unload cyclic behaviour of flax fibre-reinforced thermoplastic and thermosetting composites. Composite Structures 2018;183:309–19. https://doi.org/10.1016/j.compstruct.2017.03.077.

[10] Baley C, Gomina M, Breard J, Bourmaud A, Davies P. Variability of mechanical properties of flax fibres for composite reinforcement. A review. Industrial Crops and Products 2019:111984. https://doi.org/10.1016/j.indcrop.2019.111984.

[11] Moudood A, Rahman A, Öchsner A, Islam M, Francucci G. Flax fiber and its composites: An overview of water and moisture absorption impact on their performance. Journal of Reinforced Plastics and Composites 2019;38:323–39. https://doi.org/10.1177/0731684418818893.

[12] Omrani F, Wang P, Soulat D, Ferreira M. Mechanical properties of flax-fibre-reinforced preforms and composites: Influence of the type of yarns on multi-scale characterisations. Composites Part A: Applied Science and Manufacturing 2017;93:72–81. https://doi.org/10.1016/j.compositesa.2016.11.013.

[13] Toubal L, Cuillière J-C, Bensalem K, Francois V, Gning P-B. Hygrothermal effect on moisture kinetics and mechanical properties of hemp/polypropylene composite: Experimental and numerical studies. Polymer Composites 2016;37:2342–52. https://doi.org/10.1002/pc.23414.

[14] Cheour K, Assarar M, Scida D, Ayad R, Gong X-L. Effect of water ageing on the mechanical and damping properties of flax-fibre reinforced composite materials. Composite Structures 2016;152:259–66. https://doi.org/10.1016/j.compstruct.2016.05.045.

[15] Scida D, Assarar M, Poilâne C, Ayad R. Influence of hygrothermal ageing on the damage mechanisms of flax-fibre reinforced epoxy composite. Composites Part B: Engineering 2013;48:51–8. https://doi.org/10.1016/j.compositesb.2012.12.010.

[16] Le Duigou A, Bourmaud A, Baley C. In-situ evaluation of flax fibre degradation during water ageing. Industrial Crops and Products 2015;70:204–10. https://doi.org/10.1016/j.indcrop.2015.03.049.

[17] Nguyen-Duy C, Makke A, Montay G. A Pull-Out Test to Characterize the Fiber/Matrix Interfaces Aging of Hemp Fiber Reinforced Polypropylene Composites. In: Nguyen-Xuan H, Phung-Van P, Rabczuk T, editors. Proceedings of the International

Conference on Advances in Computational Mechanics 2017, Singapore: Springer Singapore; 2018, p. 477–84. https://doi.org/10.1007/978-981-10-7149-2_32.

[18] Malloum A, Mahi AE, Idriss M. The effects of water ageing on the tensile static and fatigue behaviors of greenpoxy–flax fiber composites. Journal of Composite Materials 2019;53:2927–39. https://doi.org/10.1177/0021998319835596.

[19] Kollia E, Saridaki X, Karagiannis D, Kostopoulos V. Effect of water aging on the mechanical properties of flax fiber/bio-based resin composites. Journal of Applied Polymer Science 2020;137:48787. https://doi.org/10.1002/app.48787.

[20] Fick A. Ueber Diffusion. Annalen Der Physik 1855;170:59–86. https://doi.org/10.1002/andp.18551700105.

[21] Langmuir-Type Model for Anomalous Moisture Diffusion In Composite Resins - Harris G. Carter, Kenneth G. Kibler, 1978 n.d. https://journals.sagepub.com/doi/10.1177/002199837801200201 (accessed January 13, 2020).

[22] Christian SJ, Billington SL. Moisture diffusion and its impact on uniaxial tensile response of biobased composites. Composites Part B: Engineering 2012;43:2303–12. https://doi.org/10.1016/j.compositesb.2011.11.063.

[23] Cherif ZE, Poilâne C, Vivet A, Ben Doudou B, Chen J. About optimal architecture of plant fibre textile composite for mechanical and sorption properties. Composite Structures 2016;140:240–51. https://doi.org/10.1016/j.compstruct.2015.12.030.

[24] Habibi M, Laperrière L, Hassanabadi HM. Effect of moisture absorption and temperature on quasi-static and fatigue behavior of nonwoven flax epoxy composite. Composites Part B: Engineering 2019;166:31–40. https://doi.org/10.1016/j.compositesb.2018.11.131.

[25] Tengsuthiwat J, Asawapirom U, Siengchin S, Karger-Kocsis J. Mechanical, thermal, and water absorption properties of melamine–formaldehyde-treated sisal fiber containing poly(lactic acid) composites. Journal of Applied Polymer Science 2018;135:45681. https://doi.org/10.1002/app.45681.

[26] Cheour K, Assarar M, Scida D, Ayad R, Gong X-L. Long-term Immersion in Water of Flax-glass Fibre Hybrid Composites: Effect of Stacking Sequence on the Mechanical and Damping Properties. Fibers Polym 2020;21:162–9. https://doi.org/10.1007/s12221-020-9494-7.

[27] Espert A, Vilaplana F, Karlsson S. Comparison of water absorption in natural cellulosic fibres from wood and one-year crops in polypropylene composites and its influence on their mechanical properties. Composites Part A: Applied Science and Manufacturing 2004;35:1267–76. https://doi.org/10.1016/j.compositesa.2004.04.004.

[28] Regazzi A, Corn S, Ienny P, Bergeret A. Coupled hydro-mechanical aging of short flax fiber reinforced composites. Polymer Degradation and Stability 2016;130:300–6. https://doi.org/10.1016/j.polymdegradstab.2016.06.016.

[29] Charlet K, Baley C, Morvan C, Jernot JP, Gomina M, Bréard J. Characteristics of Hermès flax fibres as a function of their location in the stem and properties of the derived

unidirectional composites. Composites Part A: Applied Science and Manufacturing 2007;38:1912–21. https://doi.org/10.1016/j.compositesa.2007.03.006.

[30] Chilali A, Assarar M, Zouari W, Kebir H, Ayad R. Effect of geometric dimensions and fibre orientation on 3D moisture diffusion in flax fibre reinforced thermoplastic and thermosetting composites. Composites Part A: Applied Science and Manufacturing 2017;95:75–86. https://doi.org/10.1016/j.compositesa.2016.12.020.

[31] Arnold JC, Alston SM, Korkees F. An assessment of methods to determine the directional moisture diffusion coefficients of composite materials. Composites Part A: Applied Science and Manufacturing 2013;55:120–8. https://doi.org/10.1016/j.compositesa.2013.08.012.

[32] Jiang X, Song J, Qiang X, Kolstein H, Bijlaard F. Moisture Absorption/Desorption Effects on Flexural Property of Glass-Fiber-Reinforced Polyester Laminates: Three-Point Bending Test and Coupled Hygro-Mechanical Finite Element Analysis. Polymers 2016;8:290. https://doi.org/10.3390/polym8080290.

[33] Beringhier M, Simar A, Gigliotti M, Grandidier JC, Ammar-Khodja I. Identification of the orthotropic diffusion properties of RTM textile composites for aircraft applications. Composite Structures 2016;137:33–43. https://doi.org/10.1016/j.compstruct.2015.10.039.

[34] Humeau C, Davies P, Jacquemin F. An experimental study of water diffusion in carbon/epoxy composites under static tensile stress. Composites Part A: Applied Science and Manufacturing 2018;107:94–104. https://doi.org/10.1016/j.compositesa.2017.12.016.

[35] Dana HR, Casari P, El Abdi R, Fréour S, Jacquemin F. Characterisation of the hygro-thermo-mechanical behaviour of organic matrix composites instrumented with optical fibres: A study of interfacial bonding. International Journal of Adhesion and Adhesives 2017;77:63–71. https://doi.org/10.1016/j.ijadhadh.2017.04.001.

[36] Beringhier M, Djato A, Maida D, Gigliotti M. A novel protocol for rapid identification of anisotropic diffusion properties of polymer matrix composite materials with complex texture. Composite Structures 2018;201:1088–96. https://doi.org/10.1016/j.compstruct.2018.05.142.

[37] Sinchuk Y, Pannier Y, Antoranz-Gonzalez R, Gigliotti M. Analysis of moisture diffusion induced stress in carbon/epoxy 3D textile composite materials with voids by μ-CT based Finite Element Models. Composite Structures 2019;212:561–70. https://doi.org/10.1016/j.compstruct.2018.12.041.

[38] Péron M, Célino A, Castro M, Jacquemin F, Le Duigou A. Study of hygroscopic stresses in asymmetric biocomposite laminates. Composites Science and Technology 2019;169:7–15. https://doi.org/10.1016/j.compscitech.2018.10.027.

[39] Chilali A, Assarar M, Zouari W, Kebir H, Ayad R. Analysis of the hydro-mechanical behaviour of flax fibre-reinforced composites: Assessment of hygroscopic expansion and its impact on internal stress. Composite Structures 2018;206:177–84. https://doi.org/10.1016/j.compstruct.2018.08.037.

[40] Zouari W, Assarar M, Chilali A, Ayad R, Kebir H. Numerical Modelling of the Transient Hygroscopic Behavior of Flax-Epoxy Composite. Journal of Renewable Materials 2019;7:839–53. https://doi.org/10.32604/jrm.2019.06773.

[41] Peret T, Clement A, Freour S, Jacquemin F. Numerical transient hygro-elastic analyses of reinforced Fickian and non-Fickian polymers. Composite Structures 2014;116:395–403. https://doi.org/10.1016/j.compstruct.2014.05.026.

[42] Joliff Y, Belec L, Chailan JF. Modified water diffusion kinetics in an unidirectional glass/fibre composite due to the interphase area: Experimental, analytical and numerical approach. Composite Structures 2013;97:296–303. https://doi.org/10.1016/j.compstruct.2012.09.044.

[43] Joliff Y, Belec L, Heman MB, Chailan JF. Experimental, analytical and numerical study of water diffusion in unidirectional composite materials – Interphase impact. Computational Materials Science 2012;64:141–5. https://doi.org/10.1016/j.commatsci.2012.05.029.

[44] Mercier J, Bunsell A, Castaing P, Renard J. Characterisation and modelling of aging of composites. Composites Part A: Applied Science and Manufacturing 2008;39:428–38. https://doi.org/10.1016/j.compositesa.2007.08.015.

[45] Meng M, Rizvi MJ, Le HR, Grove SM. Multi-scale modelling of moisture diffusion coupled with stress distribution in CFRP laminated composites. Composite Structures 2016;138:295–304. https://doi.org/10.1016/j.compstruct.2015.11.028.

[46] Ouled Ahmed RBA, Chatti S, Ben Daly H. Modeling of Hygrothermal Damage of Composite Materials. Mechanics of Advanced Composite Structures 2016;3:137–44. https://doi.org/10.22075/macs.2016.475.

[47] Peret T, Clement A, Freour S, Jacquemin F. Effect of mechanical states on water diffusion based on the free volume theory: Numerical study of polymers and laminates used in marine application. Composites Part B: Engineering 2017;118:54–66. https://doi.org/10.1016/j.compositesb.2017.02.046.

[48] Crank J, Crank EPJ. The Mathematics of Diffusion. Clarendon Press; 1979.

[49] De Wilde WP, Frolkovic P. The modelling of moisture absorption in epoxies: effects at the boundaries. Composites 1994;25:119–27. https://doi.org/10.1016/0010-4361(94)90005-1.

[50] Aoki Y, Yamada K, Ishikawa T. Effect of hygrothermal condition on compression after impact strength of CFRP laminates. Composites Science and Technology 2008;68:1376–83. https://doi.org/10.1016/j.compscitech.2007.11.015.

[51] Bao L-R, Yee AF. Moisture diffusion and hygrothermal aging in bismaleimide matrix carbon fiber composites—part I: uni-weave composites. Composites Science and Technology 2002;62:2099–110. https://doi.org/10.1016/S0266-3538(02)00161-6.

[52] Choi HS, Ahn KJ, Nam J-D, Chun HJ. Hygroscopic aspects of epoxy/carbon fiber composite laminates in aircraft environments. Composites Part A: Applied Science and Manufacturing 2001;32:709–20. https://doi.org/10.1016/S1359-835X(00)00145-7.

[53] Yan L, Chouw N, Jayaraman K. Flax fibre and its composites – A review. Composites Part B: Engineering 2014;56:296–317. https://doi.org/10.1016/j.compositesb.2013.08.014.

[54] Baley C, Busnel F, Grohens Y, Sire O. Influence of chemical treatments on surface properties and adhesion of flax fibre–polyester resin. Composites Part A: Applied Science and Manufacturing 2006;37:1626–37. https://doi.org/10.1016/j.compositesa.2005.10.014.

[55] Charlet K, Jernot J-P, Breard J, Gomina M. Scattering of morphological and mechanical properties of flax fibres. Industrial Crops and Products 2010;32:220–4. https://doi.org/10.1016/j.indcrop.2010.04.015.

[56] Bunsell AR. Hydrothermal Ageing of Composite Materials. Rev Inst Fr Pét 1995;50:61–7. https://doi.org/10.2516/ogst:1995006.

[57] Liu M, Wu P, Ding Y, Chen G, Li S. Two-Dimensional (2D) ATR−FTIR Spectroscopic Study on Water Diffusion in Cured Epoxy Resins. Macromolecules 2002;35:5500–7. https://doi.org/10.1021/ma011819f.

[58] Li L, Yu Y, Wu Q, Zhan G, Li S. Effect of chemical structure on the water sorption of amine-cured epoxy resins. Corrosion Science 2009;51:3000–6. https://doi.org/10.1016/j.corsci.2009.08.029.

[59] Baley C. Analysis of the flax fibres tensile behaviour and analysis of the tensile stiffness increase. Composites Part A: Applied Science and Manufacturing 2002;33:939–48. https://doi.org/10.1016/S1359-835X(02)00040-4.

[60] Monti A, El Mahi A, Jendli Z, Guillaumat L. Mechanical behaviour and damage mechanisms analysis of a flax-fibre reinforced composite by acoustic emission. Composites Part A: Applied Science and Manufacturing 2016;90:100–10. https://doi.org/10.1016/j.compositesa.2016.07.002.

[61] Célino A, Fréour S, Jacquemin F, Casari P. Characterization and modeling of the moisture diffusion behavior of natural fibers. J Appl Polym Sci 2013;130:297–306. https://doi.org/10.1002/app.39148.

[62] Affdl JCH, Kardos JL. The Halpin-Tsai equations: A review. Polymer Engineering & Science 1976;16:344–52. https://doi.org/10.1002/pen.760160512.

[63] Vaddadi P, Nakamura T, Singh RP. Transient hygrothermal stresses in fiber reinforced composites: a heterogeneous characterization approach. Composites Part A: Applied Science and Manufacturing 2003;34:719–30. https://doi.org/10.1016/S1359-835X(03)00135-0.

[64] Stamboulis A, Baillie CA, Peijs T. Effects of environmental conditions on mechanical and physical properties of flax fibers. Composites Part A: Applied Science and Manufacturing 2001;32:1105–15. https://doi.org/10.1016/S1359-835X(01)00032-X.

[65] Karalekas D, Cugnoni J, Botsis J. Monitoring of hygrothermal ageing effects in an epoxy resin using FBG sensor: A methodological study. Composites Science and Technology 2009;69:507–14. https://doi.org/10.1016/j.compscitech.2008.11.028.

[66] Changsoo Jang, Yoon S, Bongtae Han. Measurement of the Hygroscopic Swelling Coefficient of Thin Film Polymers Used in Semiconductor Packaging. IEEE Trans Comp Packag Technol 2010;33:340–6. https://doi.org/10.1109/TCAPT.2009.2038366.

[67] Glaskova-Kuzmina T, Aniskevich A, Sevcenko J, Borriello A, Zarrelli M. Cyclic Moisture Sorption and its Effects on the Thermomechanical Properties of Epoxy and Epoxy/MWCNT Nanocomposite. Polymers 2019;11:1383. https://doi.org/10.3390/polym11091383.

[68] Yang S, Kwon S, Lee MY, Cho M. Molecular dynamics and micromechanics study of hygroelastic behavior in graphene oxide-epoxy nanocomposites. Composites Part B: Engineering 2019;164:425–36. https://doi.org/10.1016/j.compositesb.2019.01.059.

[69] Péron M, Célino A, Castro M, Jacquemin F, Le Duigou A. Biocomposites with Asymmetric Stacking for the Study of Hygro-mechanical Couplings. RCMA 2019;29:243–52. https://doi.org/10.18280/rcma.290408.

[70] le Duigou A, Merotte J, Bourmaud A, Davies P, Belhouli K, Baley C. Hygroscopic expansion: A key point to describe natural fibre/polymer matrix interface bond strength. Composites Science and Technology 2017;151:228–33. https://doi.org/10.1016/j.compscitech.2017.08.028.

[71] Garat W, Le Moigne N, Corn S, Beaugrand : J, Bergeret A. Swelling of natural fibre bundles under hygro- and hydrothermal conditions: determination of hydric expansion coefficients by automated laser scanning. Composites Part A: Applied Science and Manufacturing 2020:105803. https://doi.org/10.1016/j.compositesa.2020.105803.

[72] Joffre T, Neagu RC, Bardage SL, Gamstedt EK. Modelling of the hygroelastic behaviour of normal and compression wood tracheids. Journal of Structural Biology 2014;185:89–98. https://doi.org/10.1016/j.jsb.2013.10.014.